International Journal of Fluid Machinery and Systems
Vol. 3, No. 4, October-December 2010

DOI: 10.5293/IJFMS.2010.3.4.292
ISSN (Online): 1882-9554

Original Paper (Invited)

A Numerical Study on Cavitation Suppression Using Local Cooling

Yuan-yuan Zhang, Xiao-jing Sun and Dian-gui Huang

Shanghai Institute of Applied Mathematics and Mechanics, Shanghai University,
No.149 Yanchang Road , Zhabei District, Shanghai, 200072, P.R. China,
wafumu1986@163.com, xjsun@shu.edu.cn, dghuang@shu.edu.cn

Abstract

This study strives to develop an effective strategy to inhibit cavitation inception on hydrofoils by using local cooling technique. By setting up a temperature boundary condition and cooling a small area on the upper surface of a hydrofoil, the fluid temperature around the cooling surface will be decreased and thereby the corresponding liquid saturation pressure will drop below the lowest absolute pressure within the flow field. Hence, cavitation can never occur. In this paper, a NACA0015 hydrofoil at 4° angle of attack was numerically investigated to verify the effectiveness of the proposed technique. The CFD results indicate that the cooling temperature and the cooling surface roughness are the critical factors affecting the success of such technique used for cavitation suppression.

Keywords: CFD, cavitation inception, cavitation suppression, local cooling temperature, surface roughness

1. Introduction

Cavitation is one ubiquitous engineering problem which can result in the production of noise as well as the possibility of material damage to nearby solid surfaces by the violent and catastrophic collapse of cavitation bubbles. In most practical devices, cavitation damage is very undesirable. Over the last several decades, considerable efforts from both experimental and analytical fronts have been devoted to understanding cavitation (Kubota , Wang , and Janssens et al [1]-[9]). Parenthetically, in many practical devices, cavitation damage is observed to occur in quite localized areas. This paper aims to develop an effective method of suppressing the cavitation inception on hydrofoils by cooling a selected local area of the upper surface of the hydrofoil, which usually has a low pressure and tends to turn into the beginning of the cavitation region. Since the water temperature around the selected area will be reduced due to the cooling effect, the saturation pressure of water at that location will correspondingly be decreased and thus lower than the local pressure. Hence, the cavitation inception on the hydrofoil can be delayed or even suppressed. CFD method is adopted to simulate the cavitation on a NACA0015 hydrofoil and investigate the mechanism of local cooling technique for the suppression of cavitation inception. In addition, the influence of cooling temperature and local cooling surface roughness on the cavitation suppression is also discussed in this paper.

2. Basic Equations

2.1 The volume fraction equation

The governing equations describing the cavitation process assume a two-phase three-component flow. The three components in the flow are non-condensable gas (dispersed gas), vapor and liquid (Bakir et al [10], Wang Xianfu et al [11], XiaoLi et al [12]), respectively. The relative amount of each component is described by a volume fraction scalar α which can indicate the degree of cavitation in the flow field.

The volume fraction of each component is denoted using the subscripts: v —vapour phase, l —liquid phase and d—dispersed gas phase in this paper, and the sum of all volume fractions must add up to 1, namely $\alpha_l + \alpha_v + \alpha_d = 1$. Besides, the volume fraction α is also related to the mass fractions y, the general expressions that represent their relationship can be written as: $y_d = \alpha_d \rho_d / \rho, y_v = \alpha_v \rho_v / \rho, y_l = \alpha_l \rho_l / \rho$, where the subscripts d, v, l stand for three different components, and ρ is designated as the mixture density. Similarly, $y_d + y_v + y_l = 1$. In many cavitation problems, the mass fraction associated with the non-condensable gas can be assumed to be mixed in the liquid phase with a constant y_d . Consequently on this basis, y_l and

Accepted for publication November 22 2010: Paper number O10032S
Corresponding author: Dian-gui Huang, Professor, dghuang@shu.edu.cn
This paper was presented at 2010 International Conference on Pumps and Fans, October 18-21, 2010, Hangzhou, China

y_d can be combined and treated as one phase. The volume fraction α_m is introduced by a formula: $\alpha_m = \alpha_l + \alpha_d$ and the density associated with α_m becomes:

$$\rho_{\mathrm{m}} = \frac{1}{(1-y_d)/\rho_l + y_d/\rho_d} \tag{1}$$

And the final volume-fraction equation can be shown as follows:

$$\frac{\partial}{\partial t}(\rho_m \alpha_m) + \frac{\partial}{\partial x_j}(\rho_m u_j \alpha_m) = \dot{\mathrm{S}}_l \tag{2}$$

$$\frac{\partial}{\partial t}(\rho_v \alpha_v) + \frac{\partial}{\partial x_j}(\rho_v u_j \alpha_v) = \dot{\mathrm{S}}_v \tag{3}$$

Where $\dot{S}_l = -\dot{S}_v$ have units of (kg/s) accounting for mass exchange between the vapor and liquid during cavitation. The forms of the source terms $\dot{S}_l, \dot{S}_v$ in this paper have been derived by considering the Rayleigh-Plesset equation for bubble dynamics (Bakir et al [10]).

2.2 The governing equations and turbulence model

The governing mixture equations for mass, momentum, energy can be seen in references (Bakir et al [10]). The SST turbulence model is employed to investigate the effects of turbulent mixing and its equations are not presented here while the reader can refer to the paper (Menter et al [13]) for more details.

2.3 Cavitation source term: Rayleigh-Plesset Model (Bakir et al [10])

The Rayleigh-Plesset euqation provides a physical approach to introduce the effects of bubble dynamics into the cavitation model and estimate the rate of vapor production. For a detailed introduction, see reference (Bakir et al [10]).

The cavitation model described here has been implemented in the commercial CFD code which follows a finite-volume/finite-element discretization procedure (Raw et al [14]) in the development of the linearized equations. The solution of the pressure-velocity system is based on a coupled approach (mass and momentum solved simultaneously) and implemented within an Algebraic Multigrid strategy (Hutchinson et al [15], Ruge et al [16]). All discrete equations are second-order accurate in space.

3. Numerical Investigations

3.1 Computational domain and conditions

The computational domain is sketched in Fig.1. A hydrofoil NACA0015 with a chord length C=0.14m is set at a 4°angle of att ack and placed in a water tunnel which has a height of 2C and a length of 5.5C. The far field computational boundaries are 1C ups tream of the hydrofoil leading edge and 3.5C downstream of the hydrofoil trailing edge. The fluid is flowing from left to right. Aft er a grid independence study has been carefully conducted, the eventual mesh has approximately 96105 computational cells. Figur e 2 shows an enlarged view of the grid around the hydrofoil, in which the height of the first near-wall grid cell is 1e-5m and thus yields a dimensionless y+ of around 1. Additionally, the arrow and letter A in Fig.2 specify the location where incipie nt cavitation happens and local cooling should be applied to the surface of hydrofoil.

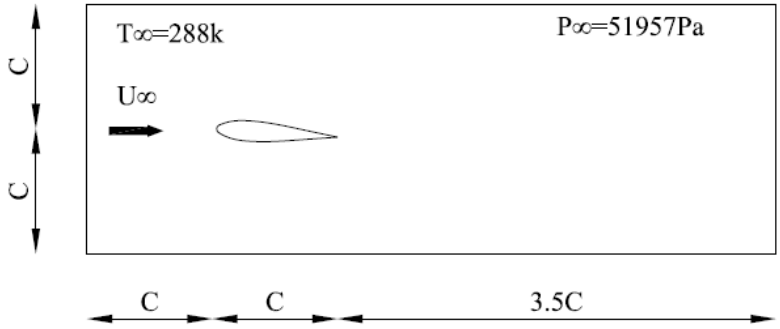

Fig. 1 Computational domain for 2D NACA0015 hydrofoil at 4°angle of attack in a water tunnel.

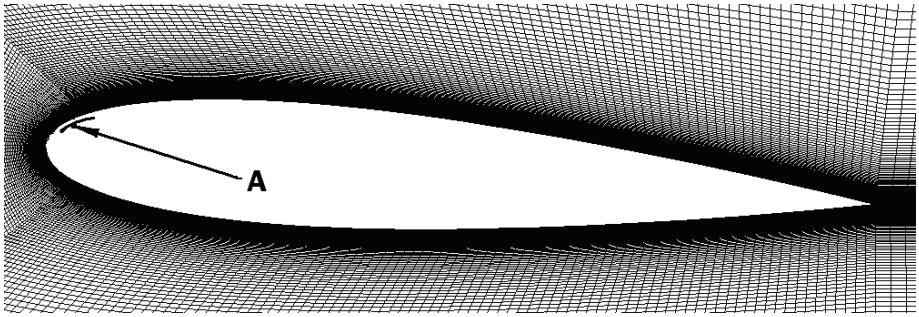

Fig. 2 Enlarged view of the mesh around NACA0015 hydrofoil at 4°angle of attack.

In all the simulations presented below, the working fluid is water at 288K. Therefore, the liquid and vapor densities are 999kg/m^3 and 0.0128kg/m^3 respectively and the saturated vapour pressure of water is 1706 Pa. The outlet absolute pressure P_∞ is set to 51957 Pa.

The NACA0015 hydrofoil is fixed at the angle of attack of 4°. During the simulation, an initial converged solution without the use of the cavitation model is first calculated meaning that a liquid volume fraction value of 1 and a gas vapor volume fraction of 0 correspond to a fully liquid state. Thereafter the cavitation model is enabled and the obtained solution has been used as an initial guess for the further cavitation simulation.

As the cavitation rate is driven by the difference between the local pressure and vapor pressure, the pressure level is then important. In order to understand the working mechanism of local cooling technique for suppression of cavitation, the formula of the incipient cavitation number $Ca = \dfrac{P_\infty - P_v}{0.5\rho_l U^2}$ must be considered and Ca needs to be determined in each simulation. The simulated cavitation attached to the hydrofoil upper surface at Ca=1.006 is presented in Fig.3 in which the distributed vaporous cavitation zone is clearly shown.

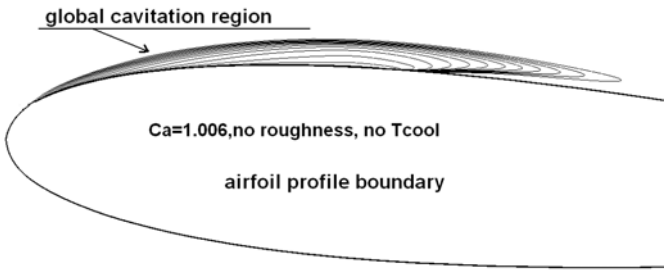

Fig. 3 Cavitation region at Ca=1.006

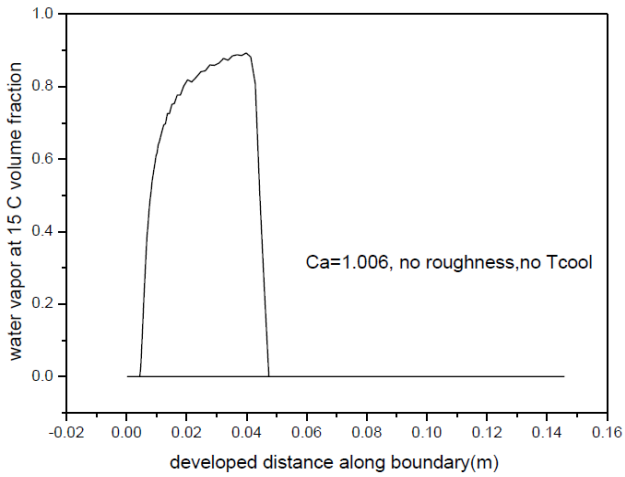

Fig. 4 The vapor volume fraction at T=15°C and Ca=1.006

It has been observed in Fig.4 that the maximum vapor volume fraction is nearly 0.9, and the length of cavitation region along the upper surface of hydrofoil is about 0.045m. In this paper, the criterion of cavitation desinence(c-s) is that the calculated volume fraction of water vapor is below 1e-06.

When the simulation is performed at Reynolds numbers $R_e = 1.32\times10^6$ and U=8.38m/s, the corresponding incipient cavitation number is 1.432. The cavitation inception happens but is just confined to the front part of the hydrofoil upper surface as seen in Fig.5, in which only part of the cavitation region is illustrated and the point M represents the beginning of the cavitation area.

The water vapor volume fraction obtained under the above conditions is shown in Fig.6. It can be seen that the maximum vapor volume fraction is 0.039, the cavitation occurrence position is approximately 0.005m downstream from the hydrofoil leading edge and the length of cavitation region is about 0.025m.

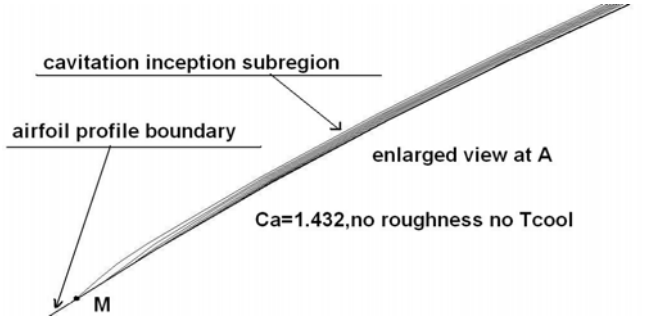

Fig. 5 Cavitation inception at Ca=1.432

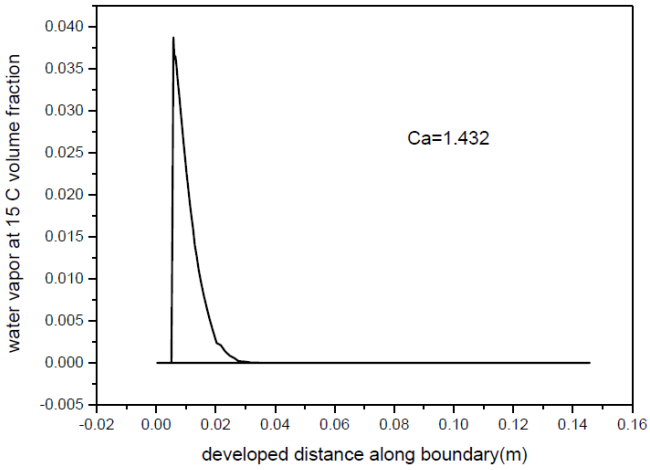

Fig. 6 The vapor volume fraction at T=15°C and Ca=1.432.

3.2 Suppression of cavitation inception by local cooling

In this section, the local cooling method is introduced and its effect on the suppression or delay of the cavitation inception is examined. It is well known that the cavitation inception happens when the local pressure falls below the saturated vapor pressure of water. Meanwhile, the saturated pressure depends on temperature (Zeng Danling et al [17]). Thus, if the cavitating hydrofoil surface is able to be cooled down to some degree below the ambient liquid temperature, the saturation pressure of the water vapor over the cooling surface will be correspondingly reduced due to the temperature gradient between the cooling surface and the surrounding water. Once the saturated vapor pressure of water can be decreased to be less than the local pressure, cavitation may not occur. In order to evaluate the effectiveness of local cooling in suppressing the cavitation, numerical investigations have been conducted based on the previous numerical model, in which a small area at about 0.005m downstream of the hydrofoil leading edge was defined as a cooling surface at a given low temperature and simultaneously the rest of hydrofoil was regarded to be adiabatic. As a result, a thermal boundary layer within the momentum boundary layer is present due to the existence of a temperature difference between the cooling surface and the surrounding water. Dimensionless Prandtl number is the ratio of momentum diffusivity to heat diffusivity and it is used as a measure of the relative effectiveness of momentum and energy transport by diffusion in the velocity and thermal boundary layers.

Heat flux at the wall was modeled using the automatic wall treatment in the SST turbulence model. Namely, the non-dimensional near-wall temperature profile follows a universal profile through the viscous sublayer and the logarithmic region (Kader et al [18]). The non-dimensional temperature T^+ is defined as:

$$T^+ = \frac{\rho C_p u^* (T_w - T_f)}{q_w} \tag{4}$$

Where T_w is the temperature at the wall, T_f is the near-wall fluid temperature, C_p is the fluid heat capacity, and q_w is the heat flux at the wall. The non-dimensional temperature distribution is then modeled as

$$T^+ = P_r y^* e^{(-\Gamma)} + [2.12 \ln(y^*) + \beta] e^{(-1/\Gamma)} \tag{5}$$

Where:

$$\beta = (3.85 P_r^{1/3} - 1.3)^2 + 2.12 \ln(P_r) \tag{6}$$

$$\Gamma = \frac{0.01 (P_r y^*)^4}{1 + 5 P_r^3 y^*} \tag{7}$$

Pr is the Prandtl number, given by $\mu c_p / \lambda$ .Where λ is the fluid thermal conductivity and $y^* = \rho u^* \Delta y / \mu$. Δy is the distance between the first and second grid points off the wall, u^* is the friction velocity depending on different near-wall treatment. Combining these equations leads to a simple form for the wall heat flux model:

$$q_w = \frac{\rho C_P u^*}{T^+} (T_w - T_f) \tag{8}$$

In the computation, the saturation pressure of the local fluid changes with the temperature gradient and the relationship (Zeng Danling et al [17]) between saturation pressure and temperature is the Clapeyron-Clausius Eq.(9):

$$\ln \frac{P_2}{P_1} = -\frac{r}{R} \left(\frac{1}{T_2} - \frac{1}{T_1} \right) \tag{9}$$

Where, the saturation pressure P_2 needs to be defined by the other variables and imported into the Rayleigh-Plesset equation. r is the latent heat of vaporization, R is the characteristic constant, and the P_1, T_1, are the quantities from the reference state: water at a temperature of 15°C.

In addition, different temperatures were given for the cooling surface area of the hydrofoil in the numerical simulation. At a given cooling temperature, the water vapor volume fraction (hereafter WVF) on both the cooling and adiabatic surface was then calculated and listed in Table 1, which clearly shows the effect of the local cooling on the cavitation suppression.

Table 1 The WVF for different Tcool and cavitation numbers

Tcool \ Ca	1.432	1.43	1.429	1.425
5°C	c-s	0.0007	0.0045	0.014
0°C	c-s	c-s	0.00137	0.0034
No Tcool	0.039	0.045	0.05	0.076

From Table 1, two tendencies have been found: at a certain cooling temperature, the decrease of cavitation number resulted in the increase of the WVF, whereas at a fixed cavitation number, the WVF decreases with decreasing the applied cooling temperature.

Figure 7 shows that at the cooling temperature of 5°C, the size of cavitation area on the hydrofoil keeps getting smaller when the cavitation number decreases.

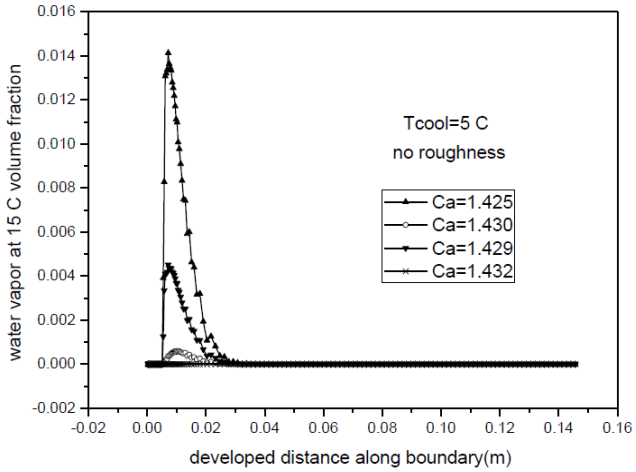

Fig. 7 The calculated WVF for different cavitation numbers at the cooling temperature of 5°C.

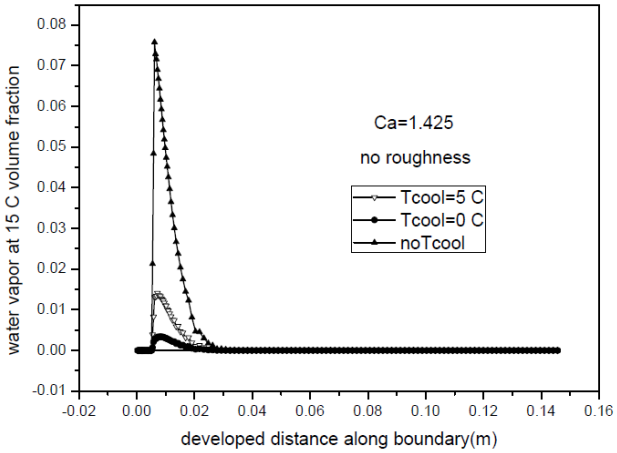

Fig. 8 The calculated WVF for different cooling temperatures at the cavitation number of 1.425.

Figure 8 shows that there is indeed an apparent effect of the temperature difference on the formation of cavitation zone on the hydrofoil surface and the calculated WVF is apparently reduced with decreasing the cooling temperature at the cavitation number of 1.425.

The results obtained so far suffice to prove that the use of the local surface cooling can effectively suppress the hydrofoil cavitation. However, this method becomes less effective at lower cavitation numbers. Furthermore, it is also worth pointing out that the rate of heat transfer is important for the cavitation suppression.

3.3 The influence of the surface roughness on suppressing cavitation inception

In the preceding work, it's found that higher temperature gradient between the cooling hydrofoil surface and the ambient water can contribute significantly to the inhibition of cavitation inception because of the heat exchange between liquid and vapor phase. However, it's not realistic to chill the hydrofoil surface down to a fairly low temperature below zero. Therefore, instead of only reducing the local hydrofoil surface temperature, another approach has also been investigated, which can quicken the heat transfer by increasing the cooling surface roughness and accordingly enhance the performance of the proposed local cooling technique. The theoretical basis of this approach is explained as follows.

The near-wall heat flux considering the roughness is defined as:

$$q_w = \frac{\rho C_P u^*}{T_B^+}(T_w - T_f) \tag{10}$$

Where q_W is the heat flux at the wall. The non-dimensional temperature distribution considering roughness is then modeled as:

$$T_B^+ = 2.12\ln(P_r \cdot y^*) + (3.85 P_r^{1/3} - 1.3)^2 - \Delta B \tag{11}$$

For sand-grain roughness h_s, the function of dimensionless roughness is $\Delta B = (1/0.41)\ln(1+0.3 C_m h_S^+)$. Where the dimensionless sand-grain roughness is defined as $h_S^+ = h_s u_\tau / \upsilon$ (Schlichting et al [19]).

The coefficient C_m has been calibrated using the experimental data of Pimenta et al [20] for a flat plate with heat transfer. The experiment was performed with air as fluid and it has been shown that a value of 0.2 is a good choice in this case (Lechner et al [21]).

Theoretically, there is more heat imported into the near-wall fluid after adding surface roughness.

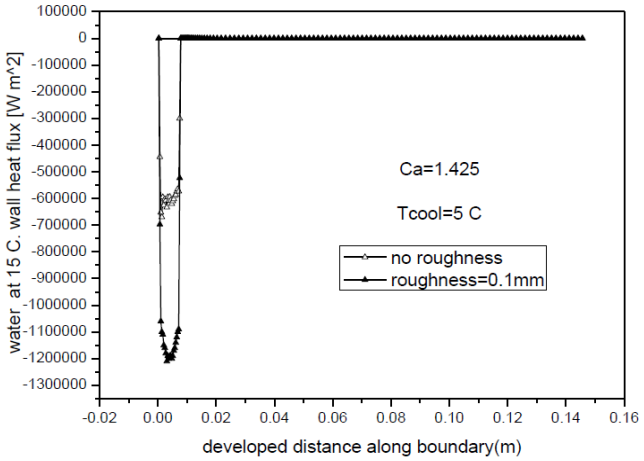

Fig. 9 The influence of roughness on the heat flux.

Figure 9 demonstrates that the wall heat flux calculated increases after introducing the roughness at a cavitation number of 1.425 and cooling temperature of 5°C. Consequently, the surface roughness can be considered to be a factor affecting the suppression of cavitation inception by the local cooling.

In Fig.10, the maximum water vapor volume fraction is found to be nearly 0.25 at Ca=1.392 when a cooling temperature as well as surface roughness are not defined for the local cooling area on the hydrofoil in the numerical model.

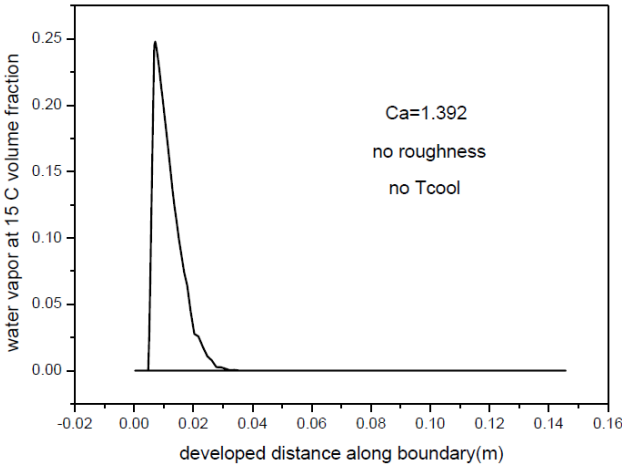

Fig. 10 The WVF at Ca=1.392 without local cooling temperature and surface roughness

Table 2 shows the values of the WVF calculated after a cooling temperature of 5°C and the surface roughness have been considered in the numerical model. It can be seen that increasing the cooling surface roughness can promote the effectiveness of the local cooling on the cavitation suppression and the cavitation region has completely disappeared when the surface roughness is increased to 0.4 mm.

Table 2 The results of WVF when Ca=1.392 and Tcool=5°C

Roughness(mm)	0.1	0.2	0.3	0.4
WVF	0.184	0.015	0.002	c-s

The comparison of the simulated WVF curve at different surface roughnesses and the given cooling temperature of 5°C is also displayed in Fig. 11 below.

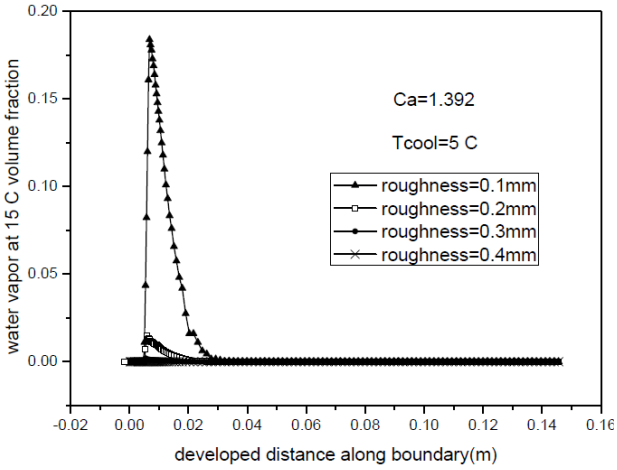

Fig. 11 Comparison of the WVF at different roughness.

3.4 The combined effect of the local cooling and increased local surface roughness

As discussed in Section 3.2 and 3.3 above, the cooling temperature and surface roughness are the most important factors for the suppression of cavitaton by the technique of local cooling and their combined effect is then investigated in this section of the paper.

Table 3 summarizes the numerical results of WVF obtained under various conditions after both of the local surface cooling temperature and roughness were taken into account in the numerical model. It has been found that under the combined effect of the local cooling temperature and surface roughness, the occurrence of cavitation can be inhibited over a wide range of cavitation numbers and the onset of cavitation is delayed until the cavitation number is reduced to 1.392.

Table 3 The combined effect of surface roughness and cooling temperature on the suppression of cavitation on hydrofoil under various conditions

U(m/s)	Tcool(°C)	Roughness(mm)	WVF	Ca
8.38	no Tcool	0	0.039	1.432
8.4	5	0.1	c-s	1.425
8.45	5	0.1	c-s	1.409
8.5	5	0.1	0.184	1.392
8.5	5	0.2	0.015	1.392
8.5	5	0.3	0.002	1.392
8.5	5	0.4	c-s	1.392
8.5	0	0.3	c-s	1.392
8.51	0	0.4	0.0047	1.389
8.51	5	0.4	0.017	1.389
8.52	0	0.9	0.016	1.385

4. Conclusions

In this paper, a numerical study is conducted to investigate the feasibility of inhibiting the hydrofoil cavitation through local cooling. Meanwhile, the effects of cooling temperature and surface roughness on the cavitation suppression have been examined in detail. On the basis of the cause of cavitation, the proposed local cooling technique is an innovative approach to suppress the hydrofoil cavitation through reducing the saturation pressure of water in the localized low-pressure region which is prone to cavitation.

Because of the local cooling effect, the temperature difference between the local cooling surface and the surrounding water can considerably reduce the value of the saturation vapor pressure at the cavitating region in the flow field. Thus, the performance of hydrofoil will not be compromised even at low cavitation numbers.

Increase of the roughness of the local cooling surface normally leads to an increase in turbulence production near the wall, which in turn can significantly enhance the heat transfer between the cooling surface and the ambient water.

Based on the numerical analysis conducted in this work, using the local cooling has been proven to be a feasible and promising method to suppress the inception of cavitation on hydrofoils.

Acknowledgments

This work was supported by National Natural Science Foundation of China (10972133) and Program for Changjiang Scholars and Innovative Research Team in University with Grant No.IRT0844.

Nomenclature

Ca	Cavitation number	*U*	freestream velocity [m/s]
Cp	Fluid heat capacity [J/K]	*u**	Friction velocity [m/s]
C	Chord length of hydrofoil [m]	u_i	Cartesion velocity [m/s]
c-s	Cavitation desinence	*WVF*	Maximum volume fraction of water vapor at 15°C
h_s	Sand-grain roughness height [m]	y_l, y_d, y_v	Mass volume fraction of liquid, dispersed phase, vapor
i, j, k	Cartesian indices	*y**	Dimensionless height from the wall ($=\rho u^* \Delta y / \mu$)
Pv	Saturation pressure [Pa]	α	Volume fraction
P_r	Prandtl number	$\alpha_l, \alpha_d, \alpha_v$	Volume fraction of liquid, dispersed phase, vapor
r	Latent heat of vaporization [J/kg]	$\rho, \rho_l, \rho_v, \rho_d$	Density of mixture, liquid, vapor, dispersed [kg/m^3]
R	Characteristic constant	υ	Dynamic viscosity of water [kg/m s]
$\overset{\bullet}{S}$	Source term [kg/s]	μ	Kinematic viscosity of water ($=\upsilon/\rho$) [m^2/s]
T	Ambient water temperature [°C]		
Tcool	Cooling temperature applied on the surface of hydrofoil [°C]		
T^+	Dimensionless temperature		

References

[1] Kubota, A., Kato, H., and Yamaguchi, H., 1992, “A New Modeling of Cavitating Flows: A Numerical Study of Unsteady Cavitation on a Hydrofoil Section,” Journal of Fluid Mechanics, Vol. 240, pp. 59-96.
[2] Wang, Y-C. and Brennen, C. E., 1994, “Shock Wave Development in the Collapse of a Cloud of Bubbles,” ASME Cavitation and Multiphase Flow Forum, FED Vol. 194, pp. 15-19.
[3] Janssens, M. E., Hulshoff, S. J., and Hoejijmakers, H. W. M., 1997, “Calculation of Unsteady Attached Cavitation,” 13th AIAA CFD Conference, Snowmass, CO, AIAA-97-1936.
[4] Fortes-Patella, R., and Reboud, J. L., 1998, “A New Approach to Evaluate the Cavitation Erosion Power,” ASME Journal of Fluids Engineering, Vol. 120, No. 2, pp. 335-344.
[5] Brennen, C. E., 1995, Cavitation and Bubble Dynamics, Oxford University Press, Oxford.
[6] Keller, A. P., and Rott, H. K., 1997, “The Effect of Flow Turbulence on Cavitation Inception,” ASME FED Meeting, Vancouver, Canada.
[7] Hsiao, C.-T., and Pauley, L. L., 1997, “Numerical Study of Tip Vortex Cavitation Inception Using a Bubble Dynamics Model,’’ ASME FED Meeting,Vancouver, Canada.
[8] Choi, J. K., and Kinnas, S. A., 1997, “Cavitating Propeller Analysis Inside of a Tunnel,” ASME FED Meeting, Vancouver, Canada.
[9] Kunz, R. F., Boger, D. A., Chyczewski, T. S., Stinebring, D. R., Gibeling, H.J., and Govindan, T. R., 1999, “Multi-Phase CFD Analysis of Natural and Ventilated Cavitation about Submerged Bodies,’’ ASME/JSME Joint Fluids Engineering Conference, San Francisco, CA, FEDSM99-3764.
[10] Bakir, F., Rey, R., Gerber, A.G., Belamri. T. and Hutchinson, B., 2004. “Numerical and Experimental Investigations of the Cavitating Behavior of an Inducer”, International Journal Rotating Machinery, Vol. 10, pp. 15-25,
[11]Wang Xianfu, 2009, “Cavitating and Supercavitating Flows Theory and Applications,” Defense industry Publishing house, pp. 165-180.
[12] XiaoLi, Zhang Xiaobin, Qiu Limin and Gan Zhihua, 2009. “Validation of full cavitation model in cryogenic fluids. ” Institute of Refrigeration and Cryogenics Zhejiang University, Hangzhou 310027, China.
[13] Menter, F.R., 1994, “Two-Equation eddy-viscosity turbulence models for engineering applications”, AIAA- Journal., Vol. 32, No. 8, pp. 1598-1605.
[14] Raw, M. J., 1985, “A new control-volume-based finite element procedure for the numerical solution of the fluid flow and scalar transport equations,” Ph.D. Thesis, University of Waterloo, Waterloo, Ontario, Canada.
[15] Hutchinson, B. R., Galpin, P. F., and Raithby, G. D., 1988, “Application of additive correction multigrid to the coupled fluid flow equations,” Numerical Heat Transfer, Vol. 13, pp. 133-147.

[16] Ruge, A. J., and Stuben, K., 1987, Multigrid Methods. In Algebraic Multigrid, Frontiers in Applied Mathematics. Ed. S. F. McCormick, Society for Industrial and Applied Mathematics, Philadelphia, Pennsylvania.
[17] Zeng Danling, Aoyue, Zhu Kexiong, Li Qingrong, 1985, “Thermaldynamic Engineering,” pp. 188-191.
[18] Kader, B.A., 1981, “Temperature and concentration profiles in fully turbulent boundary layers,” International Journal of Heat and Mass Transfer, Vol. 24, No. 9, pp. 1541-1544.
[19] Schlichting,H.,andGersten,K.,1997, “Grenzschicht-Theorie,” 9. Auflage, Springer-Verlag Berlin, Heidelberg, New York.
[20] Pimenta, M.M., Moffat, R.J. and Kays, W.M., 1975, “The Turbulent Boundary Layer: An Experimental Study of the Transport of Momentum and Heat with the Effect of Roughness,” Interim Report Stanford University, CA.
[21] Lechner, R., and Menter, F., 2004, “Development of a rough wall boundary condition for ω-based turbulence models,” Technical Report ANSYS / TR-04-04.